Behavior of reinforced concrete beams strengthened with externally bonded hybrid fiber reinforced polymer systems

Rami A. Hawileh, Hayder A. Rasheed, Jamal A. Abdalla, and Adil K. Al-Tamimi

Published Version Information

Citation: Hawileh, R. A., Rasheed, H. A., Abdalla, J. A., Al-Tamimi, A. K. (2014). Behavior of reinforced concrete beams strengthened with externally bonded hybrid fiber reinforced polymer systems. Materials and Design, 53, 972-982.

Digital Object Identifier (DOI): doi:10.1016/j.matdes.2013.07.087

Publisher's Link: http://www.sciencedirect.com/science/article/pii/S0261306913007152

Behavior of Reinforced Concrete Beams Strengthened with Externally Bonded Hybrid Fiber Reinforced Polymer Systems

Rami A. Hawileh[a,*], Hayder A. Rasheed[b], Jamal A. Abdalla[a], and Adil K. Al-Tamimi[a]

[a] *Department of Civil Engineering, American University of Sharjah, Sharjah P.O.Box 26666, UAE, Tel.: +971 6 515 2496, fax: +971 6 515 2979*
*E-mail address: rhaweeleh@aus.edu

[b] Kansas State University, Manhattan, Kansas, 66506, USA

ABSTRACT

This paper presents an experimental and an analytical investigation of the behavior of Reinforced Concrete (RC) beams strengthened in flexure by means of different combinations of externally bonded hybrid Glass and Carbon Fiber Reinforced Polymer (GFRP/CFRP) sheets. In order to obtain the mechanical properties of the hybrid sheets, multiple tensile coupon tests were conducted. In addition, an experimental program consisting of a control beam and four beams strengthened in flexure with GFRP, CFRP and hybrid FRP sheets was conducted. The series of the RC beams were tested under four point bending to study the flexural effectiveness of the proposed hybrid FRP sheets. The load-deflection response, strain readings at certain locations and associated failure modes of the tested specimens had been recorded. It is observed that the increase in the load capacity of the strengthened beams ranged from 30% to 98% of the un-strengthened control RC beam depending on the combination of the Carbon/Glass sheets. It was also observed that the ductility at failure loads of the beams strengthened with glass and hybrid sheets is higher than that with a single carbon sheet. Hence, the selection of the optimum combination of hybrid sheets can lead to a strengthening material which provides an improved ductility and strength in beam behavior. The load carrying capacity of the tested specimens was then predicted by the ACI 440.2R-08 guidelines. The predicted and measured results were in good agreement, within 5% for the control beam and for beams with one layer of strengthening

sheet and between 13%-17% for beams with two or more layers of hybrid strengthening sheets. Furthermore, an analytical model was developed to predict the load-deflection response of the tested specimens and the results were compared with the measured experimental data. The results showed that the developed analytical model predicted the response of the tested beam specimens with reasonable accuracy.

Keywords: hybrid systems; Fiber Reinforced Polymer; externally bonded sheets; flexural strengthening; Carbon; Glass.

1. Introduction

The use of externally bonded Fiber Reinforced Polymer (FRP) systems has been proven to be an effective technique to rehabilitate and strengthen deficient and deteriorated structural members [1-5]. The FRP materials are known to have high stiffness, high strength to weight ratio, resistance to corrosion and ease of installation. In this external strengthening technique, the FRP materials are attached to the tension side of RC beams or girders to carry the tensile stresses by means of the epoxy adhesive [6-8]. In general, the FRP plates are bonded to the soffit of the beams and the sheets are attached at anchorage zones to provide a locking mechanism that would increase the load carrying capacity of the structural member. It should be noted that the externally bonded systems were produced in the early 1940s [9] in which steel plates were bonded to bridge girders to carry extra tensile forces introduced by the increasing number of users and vehicles. However, the introduction of FRP materials showed better performance than the conventional methods due to the several mechanical advantages of the FRP materials.

Many experimental programs and numerical studies investigated different strengthening techniques in which multiple arrangements of FRP plates and sheets were used [10-19]. Among them, Akbarzadeh and Maghsoudi [10] experimentally investigated the performance of

continuous high-strength reinforced concrete beams externally strengthened with CFRP and GFRP sheets. The authors also developed an analytical model based on moment curvature that was able to predict the response and load-carrying capacity of the tested specimens with reasonable accuracy. It was concluded that as the number of CFRP sheets increases, the load-carrying capacity of the tested specimens increases, while the moment redistribution and ductility decrease along with a decrease in the CFRP ultimate strain at failure. Similarly, for the specimens strengthened with GFRP sheets, test results showed that by increasing the number of GFRP sheets, the moment redistribution and ductility would decrease without a significant increase in the load-carrying capacity. Zhou et al. [11] experimentally investigated the performance of reinforced concrete beams externally strengthened with friction hybrid bonded FRP (FHB-FRP) systems. The performance of the proposed system was mainly attributed to the improve bonding and sliding displacement of the CFRP sheets to the adjacent concrete surfaces. Test results have showed that debonding could be prevented by using the proposed FHB-FRP strengthening technique. In addition, the load-carrying capacity, cracking and yield loads of the beams strengthened with the FHB-FRP system outperformed specimens that were strengthened using the conventional U-Jacketing technique. A finite element model was also developed that was able to capture the response of the strengthened specimens with the proposed (FHB-FRP) system. Rabinovitch and Frostig [14] tested five strengthened and retrofitted existing reinforced concrete beams with externally bonded FRP materials with different edge wrapping configurations. The results revealed that the proposed strengthening method is suitable for repairing severely damaged reinforced concrete beams. Toutanji et al. [15] tested seven reinforced concrete beams externally strengthened with three to six layers of CFRP sheets via an organic epoxy, in addition to a control unstrengthend specimen. Their results indicated a

significant increase in the load-carrying capacity up to 170.2% of the control beam specimen. However, the ductility of the strengthened specimens has been reduced significantly. Further, the beam specimens strengthened with three and four layers of CFRP sheets failed by FRP rupture, while specimens strengthened with five and six layers of CFRP sheets failed by concrete cover delamination.

There have been some attempts to study the effect of using hybrid carbon and glass sheets as external strengthening material. Grace et al. [20] developed a uniaxial ductile hybrid FRP fabric composed of two types of carbon fibers and one type of glass fiber. Eight concrete beams were strengthened and tested under flexural load to examine the effectiveness and ductility of the developed fabric. The results were compared with similar beams strengthened with CFRP sheets, fabric, and plates. It was observed that the beams strengthened with the developed hybrid fabric achieved higher ultimate strength and ductility indexes compared to those beams strengthened with the available CFRP systems. Grace et al. [21] also developed a pseudo-ductile FRP fabric composed of carbon and glass fibers braided in three different directions (0°, 45°, and -45°). It was observed that the developed fabric offered strength, stiffness and achieved ductile pseudo plateaus similar to steel reinforcement when loaded axially or diagonally.

Xiong et al. [22] conducted a test program on the behavior of two strengthening systems namely; a conventional CFRP system as well as a hybrid CFRP/GFRP system. The beams were tested under four point bending. It was observed that the hybrid combination showed an 89.7% increase in the deflection response over the CFRP system. In addition, the hybrid system dropped by 10 and 38% in stiffness and cost compared to the carbon FRP system. Also, it was observed

that the ductility of the RC strengthened beam using the hybrid system was only 16.2% less than the reference control RC beam.

Similarly, Wu et al. [23] studied the effect of combining high strength and high modulus carbon sheets to form a new hybrid system. In addition, they conducted a full scale experimental program on fifteen RC beams strengthened with different configurations of the proposed hybrid system and tested monotonically under three point bending. Furthermore, the pre-cracking effect was also studied, and introduced at a preloading of 40% and 60% of the steel reinforcement yielding level. It was found that the best hybrid combination is using a high strength to high modulus ratio of 2:1. The use of high modulus carbon sheets in the hybrid system showed a large increase in the flexural stiffness, yielding load, ductility and reduction in the crack propagation within the tested RC beams. It was also found that the flexural capacity of the pre-cracked specimens can be fully restored to its original designed level using the externally bonded hybrid system.

Li-juan et al. [24] investigated numerically the interfacial stress between hybrid CFRP and GFRP sheets using the nonlinear finite element method. It was concluded that the hybrid FRP strengthening method could reduce interfacial shear and normal stresses at the cut-off point of the FRP sheets that would delay the initiation of debonding. They also performed a parametric study to investigate the effect of the load, elastic modulus, thickness of epoxy adhesive layer and FRP sheet width. It was observed from the results of the parametric study that interfacial stresses increase with the increase in the elastic modulus and loads, and decrease with the increase in the epoxy layer thickness. They concluded that, the width of the FRP sheet on the other hand has no significant influence on the interfacial stresses at the FRP ends.

Choi et al. [25] recently developed a fabric produced by combining carbon and glass fibers with a glass to carbon ratio of 8.8/1.0 to strengthen nonductile flexural members. They tested plain RC beams and RC beams strengthened with the produced FRP fabric sheets in four-point bending to examine the effect of the designed 8.8/1.0 volume ratio. It was observed that the strengthened beams with a glass to carbon fibers ratio of 8.8/1.0 exhibited higher strength than the unstrengthened beams by 20% and were able to sustain the ultimate loads without degradation demonstrating a pseudo-ductile behavior. They also conducted six bond tests to study the bond-shear stress between the hybrid sheet and concrete. It was observed that the bond behavior to concrete of the hybrid sheet is similar to that of the commonly used carbon sheet. It was found that the effective bond length and bond shear strength of the hybrid sheet is about 200 mm and 3 MPa, respectively.

This paper investigates experimentally and analytically the performance of RC beams externally strengthened in flexure with different combinations of CFRP and GFRP sheets. The first stage of this study was to obtain the mechanical properties of the hybrid sheets by conducting multiple tensile coupon tests on different arrangements of the hybrid sheets. Then, four RC beams strengthened with GFRP, CFRP and hybrid FRP sheets were tested under four-point bending. The load-deflection response, strain readings at certain locations and associated failure modes of the tested specimens was recorded. The results were compared with an unstrengthened control beam. Also, an analytical model was developed to predict the load-deflection response and load-carrying capacity of the beams and the results were compared with the experimentally measured values and the ACI 440.2R-08 [26] predictions.

2. Experimental program

2.1. Details of the Tested Beams

Five RC beams were cast using a single batch of Self-Consolidating Concrete (SCC) with average compressive 28-day cylinder strength of 50 MPa. The beams were 1840 mm long, 120 mm wide, 240 mm deep with 25 mm cover on top, bottom and sides. The flexural reinforcement of the beams consisted of two 10 mm diameter steel bars (No. 10, area = 154 mm^2) located at a depth of 202 mm from the compression face of the beam's cross-section, and two compression 8 mm diameter steel bars (No. 8, area = 98 mm^2) located at a depth of 37 mm from the compression face. The beams were over-reinforced for shear with 8 mm diameter (No. 8) closed stirrups spaced at 80 mm center to center to avoid shear failure. Figure 1a shows the geometry, dimensions and reinforcement details of the tested RC beams. The beams were cured for 28 days and kept in a controlled lab environment prior to testing.

The beams were loaded in four-point bending as shown in Figs. 1b-1c and tested until failure using a controlled Universal Testing Machine (UTM) that has a static loading capacity of 2500 kN. The loading was applied in terms of displacement control at a slow rate of 2mm/min to capture the propagation of cracks and response of the tested specimens. The clear span of the beams was 1690 mm and the two loading points were 567 mm apart located symmetrically about the beam's mid-span location. Electrical strain gauges were attached on the surface of the FRP sheets at mid-span to measure the FRP strains. The strain gauges were connected to a data acquisition system to record the strain readings. Uniaxial coupon tests were conducted on the steel reinforcement bars to measure their tensile mechanical properties. The average obtained elastic modulus and yield strength for the bars were 202 GPa and 540 MPa, respectively.

2.2. Test Matrix: Control and Strengthened Beams

A summary of the test matrix including the configuration of external hybrid FRP is given in Table 1. One beam was left unstrengthened to serve as a control specimen (B) and the

remaining four beams were strengthened on the tension side at the soffit of the RC beams with externally bonded Carbon (BC), Glass (BG), Glass-Carbon (BGC), and Glass-Carbon-Glass (BGCG) sheets, respectively. All the installed FRP sheets have a width of 112.5 mm and length of 1520 mm (90% of the beam's span length), centered along the length of the beams as shown in Fig. 1b. The dry CFRP and GFRP sheets used in the experimental program were "SikaWrap®-300 C/60" and "ReCon Wrap GF", respectively. Sikadur®-330 two parts epoxy adhesive was used to attach each FRP layer. The Sikadur®-330 has a tensile strength, modulus of elasticity and elongation at break as reported by the manufacturer of 30 MPa, 4.5 GPa and 0.9%, respectively.

2.3. Material Properties of the Fibrous Sheets

The manufacturer's mechanical properties (modulus of elasticity, tensile strength, and elongation) of the dry carbon and glass fiber sheets are given in Table 2, respectively.

It should be noted that the final composite laminate product properties are much lower than those of the dry fiber characteristics, as reported by Okeil et al. [27] due to the effects of the epoxy adhesive. In order to obtain the mechanical properties of the bonded sheets, sixteen tensile coupon tests were conducted at a displacement rate of 2 mm/min using a 100 kN universal testing machine in accordance with the ASTM: D 3039/D 3039M-08. The FRP laminate composite samples had the same arrangement as the sheets used to strengthen the RC beam specimens. Each coupon specimen had a length and width of 250 and 40 mm, respectively. The measured average composite laminate thickness for each composite type is provided in Table 3. Four coupon tests were made for each arrangement and the average tensile results are presented in Table 3.

Figure 2 shows representative stress-strain relationships of the CFRP, GFRP and hybrid FRP sheets. It is clear from Table 3 and Fig. 2 that the carbon fiber material exhibited higher tensile strength and modulus of elasticity, and lower rupture strain compared to that of the glass fibers. When the carbon and glass fibrous materials are bonded together in a composite laminate, progressive failure initiates in the carbon fibers that has a lower rupture strain. Figure 2 depicts the phenomenon of the hybrid system when carbon and glass sheets work together. As expected , when glass and carbon fiber sheets are stacked together with epoxy adhesive, the glass fibers that have higher elongation compared to the carbon fibers will stand the extra deformation due to the initiation of rupture in the carbon fibers at the onset of a drop in the stress-strain curve as shown in Figure 2. The consequent fluctuating in the load is caused by the gradual rupture of the carbon fibers. The glass fibers will retard the progress of fracture of the carbon fibers, which will lead to a significant increase in the elongation of the composite laminate with an interesting ductile-bilinear behavior similar to that of the steel reinforcement, hence providing both strength and pseudo-ductility at the same time.

2.4. Strengthening Technique

The strengthening procedure used to bond the FRP sheet to concrete involved surface preparation, epoxy resin undercoating, application of the FRP sheet and epoxy overcoating. Special consideration was given to surface preparation before applying the epoxy adhesive. Uniform mechanical grinding was used to roughen the surface of the concrete substrate and remove the surface grease and smoothness. The free particles and dust on the beams' concrete surfaces were vacuum-cleaned with compressed air after grinding. Once the exposed surface had been prepared, the two parts Sikadur®-330 epoxy adhesive was mixed in accordance with the manufacturer's instructions and applied to the concrete surface using a spatula. For the beams

strengthened with the hybrid sheets, the second FRP layer was applied on the surface of the first FRP layer which was overcoated with the epoxy adhesive. The sheets were applied with a constant pressure with rollers to ensure complete bond between the concrete and the CFRP sheets and avoid any entrapped air bubbles at the epoxy/concrete or epoxy/sheet interface. The beam specimens were allowed to cure under laboratory conditions for at least 2 weeks prior to testing.

3. Results and Discussion

The obtained experimental results are presented in the subsequent sections in terms of the observed failure modes, load versus mid-span deflection, load-FRP strain relationships at mid-span and beams' ductility.

3.1. Failure Modes

The tested RC beams showed different local and global failure modes including concrete crushing, flexure cracks, debonding, and delamination. Figure 3 shows the tested specimens at failure. Table 4 provides the measured ultimate load-capacity and a summary of the type of final failure for each beam specimen.

The control beam failed in a flexural mode by yielding of the flexural steel followed by crushing of the concrete (compression failure) at mid-span as shown in Fig. 3 (a). The BC beam specimen failed by steel yielding followed by debonding of the externally bonded CFRP sheet. It should be noted that the debonding of the CFRP sheet is due to the development of vertical shear cracks from both sides of the beam in the shear span close to the location of the point loads. The BG beam specimen failed by steel yielding followed by GFRP debonding in the vicinity of the mid-span that caused two major flexural cracks to develop and concrete crushing at the loading support to take place, as shown in Fig. 3 (c). Similarly, the BGC beam specimen failed by steel

yielding followed by partial debonding of the FRP hybrid sheets that caused a major flexural crack to develop and concrete crushing below the loading supports as shown in Fig. 3 (d). The BGCG specimen failed interestingly in a flexural mode by steel yielding followed by concrete crushing in the vicinity of the constant moment region between the two loading supports as shown in Fig. 3 (e). Furthermore, FRP debonding during testing was not observed in specimen BGCG.

3.2. Load-Deflection Responses

Figure 4 shows the load-mid-span deflection responses obtained from the tests. Table 5 summaries the experimental results in terms of the ultimate load (P_u), mid-span deflection at yielding of the flexural steel (δ_y), deflection at ultimate load (δ_u), and deflection at failure load (δ_f). The ultimate load and the maximum deflection of the control (B) and the CFRP (BC) beam specimens are used as benchmarks for measuring the performance of other beams. Table 5 also provides the percent decrease of deflection at ultimate loads ($\%\delta_u$) compared to that of the control beam, percent increase of deflection at ultimate loads ($\%\delta_u$) compared to that of the BC specimen, and the percent decrease of deflection at failure (δ_f) compared to that of the control beam.

It is clear from Fig. 4 and Table 5 that the strengthened beams have larger post cracking stiffness and load capacity than those of the control beam. It is observed that the increase in the ultimate (peak) load of the strengthened beams ranged from 30% to 98% of the un-strengthened control RC beam. Such increase in the load-carrying capacity is in agreement with other experimental studies [1-2, 8, 10, 11, 14-15]. In addition, the RC beams strengthened with hybrid sheets achieved higher ultimate load capacities than both RC beams strengthened with a single layer of CFRP or GFRP sheets. This was also observed in the experimental study of Grace et al. [20-21] and Xiong et al. [22]. Among the two beams (BC and BG) strengthened with one layer of FRP

sheet, the BC specimen achieved a higher load capacity compared to the BG specimen but failed at a lower mid-span deflection (less ductile). The beams strengthened with the hybrid sheets (BGC and BGCG) achieved higher maximum load and deformation at failure than those of the BC specimen. The BGCG specimen achieved the highest ultimate load and mid-span deflection (highest ductility) among the strengthened beam specimens. This shows that strengthening RC beams with hybrid FRP sheets would achieve a higher load capacity and ductility than those strengthened with conventional CFRP sheets. Such observations are in agreement with the findings observed by grace et al. [20-21] when strengthening RC beams with externally bonded FRP fabric composed of carbon and glass fibers braided in three different directions of 0°, 45°, and -45°, respectively.

3.3. Load-FRP Strain Relationships

Strain readings in the FRP at mid-span were recorded from the attached strain gages during testing using a data acquisition system. Figure 5 shows the load versus FRP strain for the BC and hybrid (BGC and BGCG) strengthened specimens. The FRP strain at failure for the BC, BGC, and BGCG specimens is 0.70%, 1.64%, and 1.11%, respectively. This indicates that 41.18%, 63.08%, and 39.64% of the capacity of the BC, BGC, and BGCG laminates was utilized. The BGCG FRP strain at failure was lower than that of the BGC specimen due to concrete crushing (flexural failure) in the constant moment region.

3.4. Ductility Indices

An attempt is made to estimate and quantify the ductility of the tested RC beams from the load-deflection relationships shown in Fig. 4. The mid-span deflection value at yielding of the flexural steel (δ_y) is used as a reference benchmark to define ductility of the tested specimens. In this study, the ductility is evaluated by computing the deflection ductility indices at ultimate load (

$\mu_{\Delta u} = \frac{\delta_u}{\delta_y}$) and failure load ($\mu_{\Delta f} = \frac{\delta_f}{\delta_y}$), respectively. The δ_y, δ_u, and δ_f values are shown in Table 5 and the calculated ductility indices are listed in Table 6. Table 6 also provides the ductility ratios of the tested specimens to those of the control (B) and BC specimens.

It is found from Table 6 that the ductility at ultimate and failure loads of the externally strengthened RC beams with FRP and hybrid FRP laminates are less than that of the control beam by 20-54% and 13-29%, respectively. The ductility at failure loads of the beams strengthened with glass and hybrid sheets (BG, BGC, and BGCG) is higher than that with a single carbon sheet (BC). The failure ductility of the beam strengthened with a single glass sheet (BG) is the highest among all the strengthened beams. In addition, the BGCG specimen achieved failure ductility higher than that of the BGC specimen by 17.8%. In conclusion, the beams strengthened with hybrid sheets have a higher strength and ductility than the beam strengthened with a single carbon sheet.

4. The predictions of ultimate load-carrying capacity based on ACI 440.2R-08

The nominal moment strength of the tested beam specimens is computed according to the ACI 440.2R-08 [26] design guidelines as follows:

$$M_n = A_s f_s\left(d - \frac{\beta_1 c}{2}\right) + \psi_f A_f f_{fe}\left(h - \frac{\beta_1 c}{2}\right) \quad (1)$$

where A_s and f_s are the cross-sectional area and stress of the steel reinforcement at section failure; d is the effective depth measured from the top compression fiber to the centroid of flexural steel reinforcement; β_1 is the depth factor of the rectangular stress block; c is the depth of the neutral axis; ψ_f is an additional reduction factor applied to the flexural contribution of the FRP reinforcement to account for bond deterioration and other uncertainties inherited in FRP; A_f and f_{fe} are the cross-sectional area and effective stress in the FRP sheets; and h is the depth of the

member. In addition, the design procedure limits the effective strain value in the FRP (ε_{fe}) to the debonding FRP strain (ε_{fd}) using Eq. 2 to check if intermediate crack-induced debonding mechanism failure mode governs.

$$\varepsilon_{fe} \le \varepsilon_{fd} = 0.41\sqrt{\frac{f'_c}{nE_f t_f}} \le 0.9\varepsilon_{fu} \quad (2)$$

where n is the number of FRP sheets, f'_c is the concrete compressive strength, E_f is the elastic modulus of FRP, and t_f is the nominal thickness of FRP laminate. It should be noted that the values listed in Table 3 of the measured and obtained material properties for the coupon tests are used herein to predict the nominal load capacity of the beam specimens. The ultimate load capacity of the control beam (B) is computed according to the ACI 318-08 [28] design guidelines.

Table 7 compares the measured and predicted ultimate load capacity of the tested beam specimens. The predicted strength utilized the as-measured material properties. Table 7 also provides the ratio of the predicted to the measured ultimate load capacity. It is clear from Table 7 that the predicted results for the control beam (B), BC and BG are very close to the measured experimental values with a maximum deviation of 5%. The ACI 440 provisions give slightly conservative estimates of the ultimate load capacity (P_u) for the hybrid specimens by margins of 13% and 17% for the BGC and BGCG specimens, respectively.

5. Analytical Model and Verifications

A nonlinear analytical model is developed to analyze RC beams strengthened with hybrid FRP laminates up to failure, Figure 6-8. The well-known incremental deformation technique is used for section analysis using 1000 thin concrete layers to locate the neutral axis for each top compression fiber strain using strain compatibility, force and moment equilibrium, Figure 9. The

resulting moment-curvature response is numerically integrated to yield the load-mid-span deflection behavior using 50 beam segments along half the span, Figure 10.

$$\Delta = \int_0^{L/2} x\,\phi(x)\,dx = \sum_{i=1}^{n} \left(\frac{\phi_i + \phi_{i+1}}{2}\right)(x_{i+1} - x_i)\left(\frac{x_i + x_{i+1}}{2}\right) \qquad (3)$$

The predicted failure modes in the analysis are the typical flexural failures of *FRP rupture* when the CFRP sheet reaches its ultimate strain, *FRP debonding* when the FRP strain reaches that of ε_{fd} from equation (2) above or *concrete crushing* after yielding of the tension steel when the extreme compression fiber strain reaches 0.003. Once the CFRP reaches rupture by attaining the smaller of ε_{fu} and ε_{fd} which represents the early failure due to the stress concentration at the intermediate induced cracking, the CFRP sheet is entirely removed from the analysis leaving just the GFRP sheet(s) and causing a drop in the load-deflection response.

Figure 11 presents the experimental and predicted response load versus mid-span deflection curve for the unstrengthened control beam, while Figure 12 presents the experimental and predicted response curves for the beams externally strengthened with FRP laminates. It is evident from Figure 11 that the two curves are corresponding reasonably well. The analytical failure mode is by yielding of the tension steel followed by concrete crushing. Figure 12a shows the experimental and the analytical load-deflection results of Beam BC with a CFRP sheet only. It can be seen from Figure 12a that the two results are in a very good agreement. The analytical failure mode is debonding of the CFRP sheet ($\varepsilon_{fd} = 0.41\sqrt{\frac{50}{119.25x1000x0.348}} = 0.0142$, see Table 3) which matches the experimental observation. Figure 12b demonstrates the comparison of the experimental response and the analytical prediction for Beam BG with a single GFRP sheet. The excellent correspondence between the two curves is evident. The analytical failure mode is by concrete crushing which is similar to the concrete crushing observed under the point

loads even though local debonding failure is evident experimentally (Figure 3c). The comparison between the test response and analysis response for Beam BGC with a hybrid GFRP and CFRP layers is shown in Figure 12c. The two responses are in excellent agreement with each other. The analytical failure mode is first partial debonding of the CFRP in the hybrid layer (ε_{fd} = $0.41\sqrt{\frac{50}{86.3x1000x0.7}}$ = 0.0118, see Table 3) upon which the CFRP layer is completely removed, yielding a drop in the load-deflection response similar to the experimental observation, followed by concrete crushing similar to the experimental concrete crushing observed under the point loads, (Figure 3d), with partial debonding also evident experimentally. Figure 12d illustrates the correspondence between the experiment and analysis results for Beam BGCG with a hybrid GFRP-CFRP-GFRP laminate. The analytical failure mode started by partial debonding of the CFRP sheet ($\varepsilon_{fd} = 0.41\sqrt{\frac{50}{65.25x1000x1.052}}$ = 0.0111, see Table 3) upon which the CFRP layer is completely removed, yielding a drop in the load-deflection response. The progressive failure ended by debonding of the remaining two Glass layers at ($\varepsilon_{fd} = 0.41\sqrt{\frac{50}{2x34.13x1000x0.352}}$ = 0.0187, see Table 3) unlike the concrete crushing failure observed experimentally. Nevertheless, it is important to note that the extreme compression fiber strain at failure was 0.0028 which is very close to the 0.003 strain used by ACI to indicate concrete crushing.

6. Conclusions

Experimental and analytical results to investigate the behavior of RC beams strengthened in flexure by means of different combinations of externally bonded hybrid GFRP and CFRP sheets are presented. Four beams externally strengthened in flexure with GFRP, CFRP, and hybrid combinations of GFRP/CFRP sheets, in addition to an unstrengthened reference beam were

tested under four point bending and the flexural effectiveness of the proposed strengthening technique with hybrid FRP sheets were investigated. It is observed that the ultimate load-carrying capacity using ACI440.2R-08 is close to the experimentally measured values. Also the analytical model predicts the behavior of the tested beams very accurately. The following conclusions are obtained:

1) The increase in the load capacity of the strengthened beams ranged from 30% to 98% of the un-strengthened control RC beam depending on the combination of the Carbon/Glass sheets.
2) The ductility at failure for the beams strengthened with glass and hybrid sheets is higher than that with a single carbon sheet. The ductility at failure of the beam strengthened with a single glass sheet is the highest among all the strengthened beams.
3) The use of hybrid systems combines the lower stiffness of the GFRP sheets with the high strength of the CFRP sheets to result in a material, which provides an improved strength and ductility in beam behavior as observed in BGC and BGCG beams.
4) From the reading of the strains in the FRP, around 40% or more of the FRP strength have been utilized. Specifically, 41.18%, 63.08%, and 39.64% of the capacity of the BC, BGC, and BGCG laminates were utilized, respectively.
5) The ACI 440 provisions gave very accurate prediction of the ultimate load capacity for the beams with one layer of strengthening sheet (BC and BG) but slightly conservative estimates of the ultimate load capacity for the hybrid specimens by margins of 13% and 17% for the BGC and BGCG specimens, respectively. It can be concluded that, ACI prediction is less accurate for hybrid specimens and also as the number of strengthening layers increases.

6) The failure modes for the tested beam specimens showed different local and global failure characteristics including concrete crushing, flexural cracks, debonding, and delamination.

Acknowledgement

The research presented in this paper has been sponsored by the American University of Sharjah. Their support is gratefully acknowledged. In addition, the authors would like to thank and acknowledge SIKA for supplying CFRP Wraps and CONMIX for supplying GFRP Wraps along with their adhesives. Their support is highly appreciated. The authors would like to also acknowledge the help of Eng. Mohannad Nasser, Basel Al Saati, Rafik Jabbour, Mais Shaaban and Farah Efara for their help in conducting the tests. The views and conclusions, expressed or implied, in this document are those of the authors and should not be interpreted as those of the sponsor.

References

[1] Meier U. (1987).Bridge repair with high performance composite materials. Material und Technik 1987; 4: 125-128.

[2] Arduini M, Tommaso A, Nanni A. Brittle failure in FRP plate and sheet bonded beams. ACI Struct J 1997; 94(4), 363-370.

[3] Larson K, Peterman R, Rasheed H. Strength-fatigue behavior of fiber reinforced polymer strengthened prestressed concrete T-beams. J Compos for Constr ASCE 2005; 9(4), 313-326.

[4] Rasheed H, Larson K, Peterman R. Analysis and design procedure for FRP-strengthened prestressed concrete T-Girders considering strength and fatigue. J. Compos for Constr ASCE 2006; 10(5), 419-432.

[5] Rasheed HA, Harrison RR, Peterman RJ, Alkhrdaji T. Ductile Strengthening Using Externally Bonded and Near Surface Mounted Composite Systems. Composite Structures 2010; 92(10): 2379-2390.

[6] Hutchinson AR, Rahimi H. Behaviour of reinforced concrete beams with externally bonded fibre resin-forced plastics. Proc. of the 5th International Conference on Struct. Faults and Repairs, University of Edinburgh, July1993, Forde (Ed.), Vol. 3, Engineering Technics Press, Edinburgh, UK, pp. 221-228.

[7] Ahmed O, Van Gemert D. Behaviour of RC beams strengthened in bending by CFRP laminates. Proc., 8th Int. Conf. on Struct. Faults and Repairs, Engineering Technics Press 1999, Edinburgh, U.K.

[8] Fanning P, Kelly O. Ultimate response of RC beams strengthened with CFRP plates. J Compos for Constr ASCE 2001; 5(2), 122-127.

[9] Asplund O. Strengthening Bridge slabs with grouted reinforcement. J Am Concr Inst 1949; 20(6):397–406.

[10] Akbarzadeh H, Maghsoudi AA. Experimental and analytical investigation of reinforced high strength concrete continuous beams strengthened with fiber reinforced polymer. Mater Des 2010; 31(3): 1130-1147.

[11] Zhou Y, Gou M, Zhang F, Zhang S, Wang D. Reinforced concrete beams strengthened with carbon fiber reinforced polymer by friction hybrid bond technique: Experimental investigation. Mater Des 2013; 50: 130-139.

[12] Doran B, Koksal HO, Turgay T. Nonlinear finite element modeling of rectangular/square concrete columns confined with FRP. Mater Des 2009; 30(8): 3066-3075.

[13] Wu YF, Huang Y. Hybrid bonding of FRP to reinforced concrete structures. J Compos Constr 2008; 12(3): 266–73.

[14] Rabinovitch O, Frostig Y. Experiments and analytical comparison of RC beams strengthened with CFRP composites. Composites: Part B 2003; 34: 663–77.

[15] Toutanji H, Zhao L, Zhang Y. Flexural behavior of reinforced concrete beams externally strengthened with CFRP sheets bonded with an inorganic matrix. Eng Struct 2006; 28: 557–66.

[16] Hawileh RA, El-Maaddawy TA, Naser Z. Nonlinear finite element modeling of concrete deep beams with openings strengthened with externally-bonded composites. Mater Des 2012; 42: 378-387.

[17] Ahmed A, Fayyadh MM, Naganathan S, Nasharuddin K. Reinforced concrete beams with web openings: A state of the art review. Mater Des 2012; 40: 90-102.

[18] Tamimi A, Hawileh R, Abdalla JA, Rasheed H. Effects of ratio of CFRP plate length to shear Span and end anchorage on flexural behavior of SCC R/C beams. J Compos for Constr ASCE 2001; 15(6): 875-1002.

[19] Hawileh R, Abdalla JA, Tamimi A. Flexural performance of strengthened RC beams with CFRP laminates subjected to cyclic loading. Key Engineering Materials 2011; 471-472: 697-702.

[20] Grace N, Abdel-Sayed G, Ragheb W. Strengthening of concrete beams using innovative ductile fiber-reinforced polymer fabric. ACI Struct J 2002; 99(5), 692-700.

[21] Grace N, Ragheb W, Abdel-Sayed G. Developing and modeling of new ductile FRP systems for strengthening concrete structures. Proc. of the IASTED International Conference on Applied Simulation and Modelling 2004; 383-391.

[22] Xiong G, Yang J, Ji Z. Behavior of reinforced concrete beams strengthened with externally bonded hybrid carbon fiber-glass fiber sheets. J Compos for Constr ASCE 2004; 8(3): 275-278.

[23] Wu Z, Shao Y, Iwashita K, Sakamoto K. Strengthening of preloaded RC beams using hybrid carbon sheets. J Compos for Constr ASCE 2007; 11(3), 299-307.

[24] Li-juan L, Yong-chang G, Pei-yan H, Feng L, Jiang Z. Interfacial stress analysis of RC beams strengthened with hybrid CFS and GFS. Constr Build Mater 2009; 23(6), 2394-2401.

[25] Choi D, Kang T, Ha S, Kim K, Kim W. Flexural and bond behavior of concrete beams strengthened with hybrid carbon-glass fiber-reinforced polymer sheets. ACI Struct J 2011; 108(1): 90-98.

[26] ACI Committee 440. Guide for the design and construction of externally bonded FRP systems for strengthening concrete structures (ACI 440.2R-08). American Concrete Institute 2008, Farmington Hills, MI, 45 pp.

[27] Okeil AM, El-Tawil S, Shahawy M. (2001). Short-term tensile strength of carbon fiber-reinforced polymer laminates for flexural strengthening of concrete girders. ACI Struct J 2001; 98(4), 212-220.

[28] ACI Committee 318. Building Code requirements for structural concrete and Commentary. American Concrete Institute 2008, Farmington Hills, MI, 473 pp.

List of Tables:

Table 1. Test Matrix

Name	Description
B	Control Beam
BC	One layer of CFRP
BG	One layer of GFRP
BGC	One layer of GFRP and one layer of CFRP bonded in sorted order
BGCG	One layer of GFRP, one layer of CFRP, and one layer of GFRP bonded in sorted order

Table 2. Manufacturer's mechanical properties

FRP Sheet	Modulus of Elasticity (GPa)	Ultimate tensile strength (MPa)	Strain at rupture (%)
Carbon	230	3450	1.5
Glass	72	3400	4.5

Table 3. Measured Mechanical Properties of Different FRP Laminates

FRP Designation	Measured Thickness (mm)	Tensile Strength (MPa)	Modulus of Elasticity (GPa)	Elongation (%)
C	0.348	2089.4	119.25	1.7
G	0.352	786.5	34.13	3.5
GC	0.700	1622.7	86.30	2.6
GCG	1.052	1186.9	65.25	2.8

Table 4. Ultimate load capacity and mode of failure

Specimen	**P_u (kN)**	**Mode of Failure**
B	58.78	Flexural (Steel yielding, concrete crushing)
BC	92.44	Steel yielding followed by FRP debonding
BG	76.84	Steel yielding followed by Local FRP debonding and concrete crushing at loading support
BGC	107.59	Steel yielding followed by FRP partial debonding, major flexural crack and concrete crushing at loading support
BGCG	116.41	Flexural (Steel yielding, concrete crushing)

Table 5. Summary of ultimate load and deflections

Specimen	P_u (kN)	% P_u Increase over B	% P_u Increase over BC	δ_y (mm)	δ_u (mm)	% δ_u Decrease over B	% δ_u Increase over BC	δ_f (mm)	% δ_f Decrease over B
B	58.78	-	-	9.36	32.74	-	76.50	33.75	-
BC	92.44	57.26	-	8.59	18.55	43.34	-	19.39	42.55
BG	76.84	30.72	-16.88	7.40	20.69	36.81	11.54	23.21	31.23
BGC	107.59	83.04	16.38	7.80	15.75	51.89	17.78	20.10	40.44
BGCG	116.41	98.04	25.93	8.86	14.11	56.90	31.47	26.90	20.30

Table 6. Summary of ductility indices at ultimate and failure loads

Specimen	$\mu_{\Delta u}$	Ratio to B specimen	Ratio to BC specimen	$\mu_{\Delta f}$	Ratio to B specimen	Ratio to BC specimen
B	3.50	1.00	1.62	3.61	1.00	1.60
BC	2.16	0.62	1.00	2.26	0.63	1.00
BG	2.80	0.80	1.29	3.14	0.87	1.39
BGC	2.02	0.58	0.94	2.58	0.71	1.14
BGCG	1.59	0.46	0.74	3.04	0.84	1.35

Table 7. Comparison of predicted ultimate load capacity with experimental results

Specimen	P_u (kN)	P_u Predicted	$(P_u)_{pred.}/(P_u)_{exp.}$
B	58.78	58.85	1.00
BC	92.44	88.03	0.95
BG	76.84	74.46	0.97
BGC	107.59	93.98	0.87
BGCG	116.41	96.25	0.83

List of Figures:

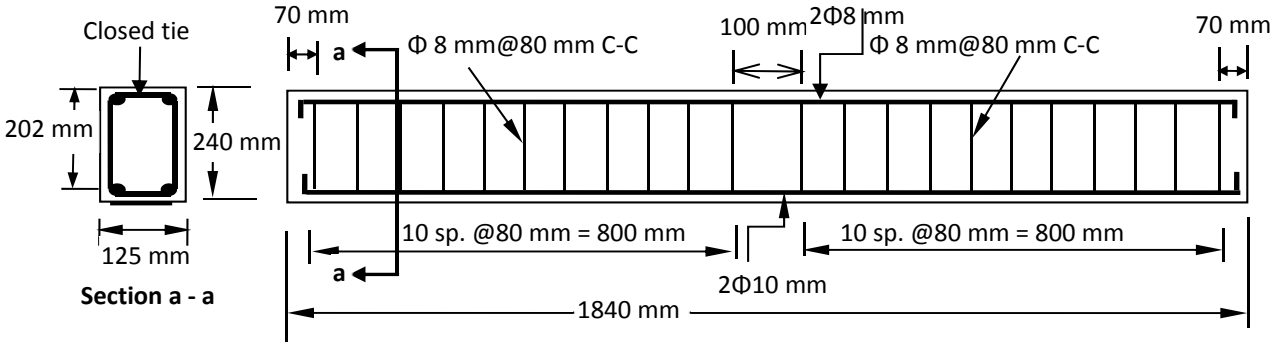

Fig. 1a. Longitudinal and cross-section reinforcement details

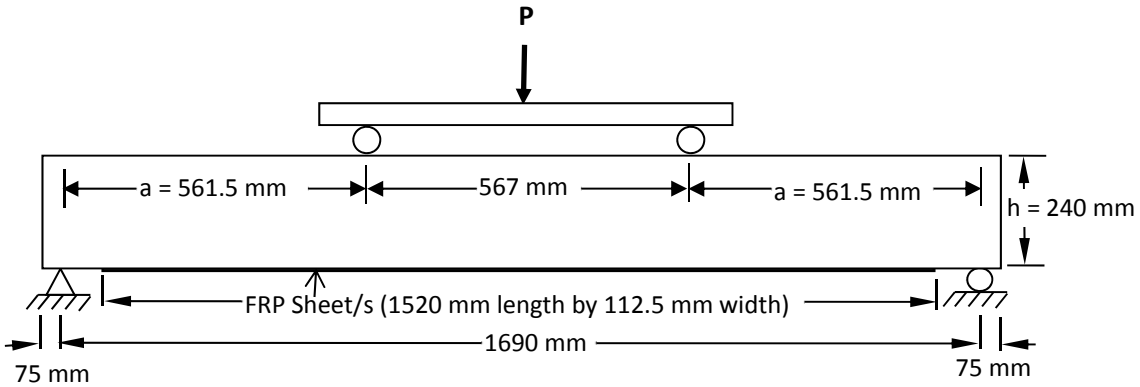

Fig. 1b. Details of tested Beams

Fig. 1c. Test Setup

Fig. 1. Details of strengthening technique and load condition

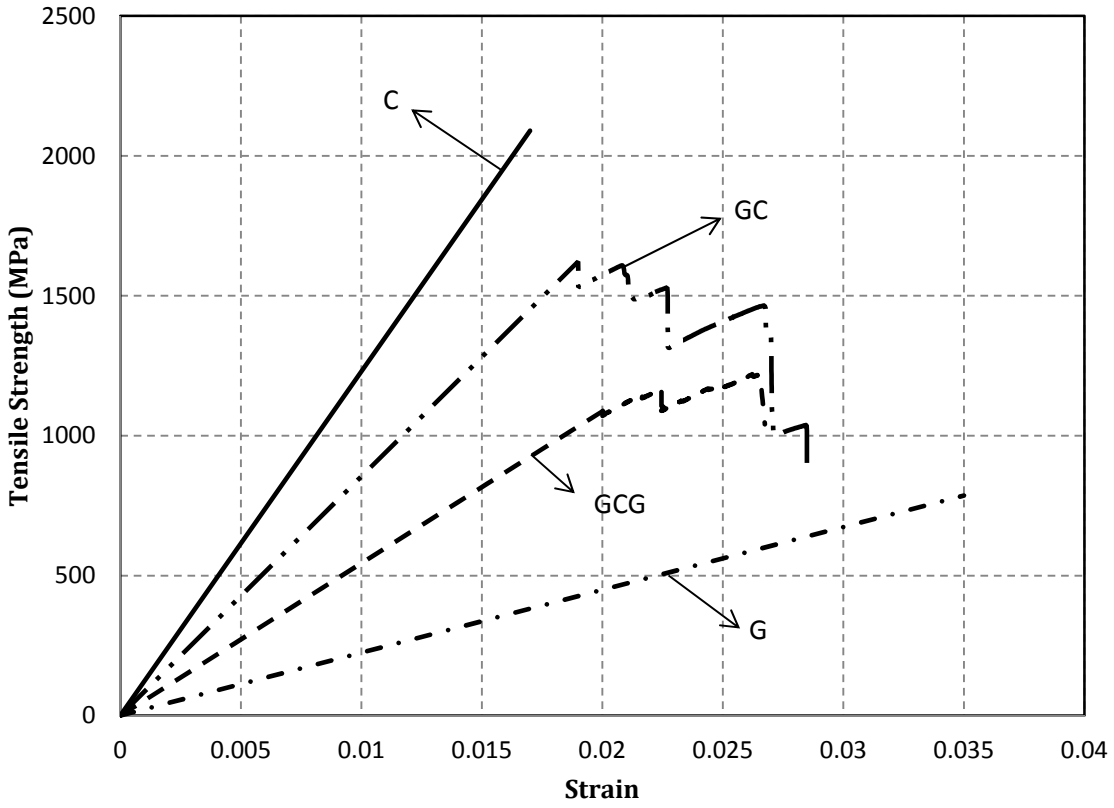

Fig. 2. Measured stress-strain curves for FRP and hybrid sheets

(a) Control Beam (B) at failure

(b) BC Beam at failure

(c) BG Beam at failure

(d) BGC Beam at failure

(e) BGCG Beam at failure

Fig. 3. Tested Beams at Failure

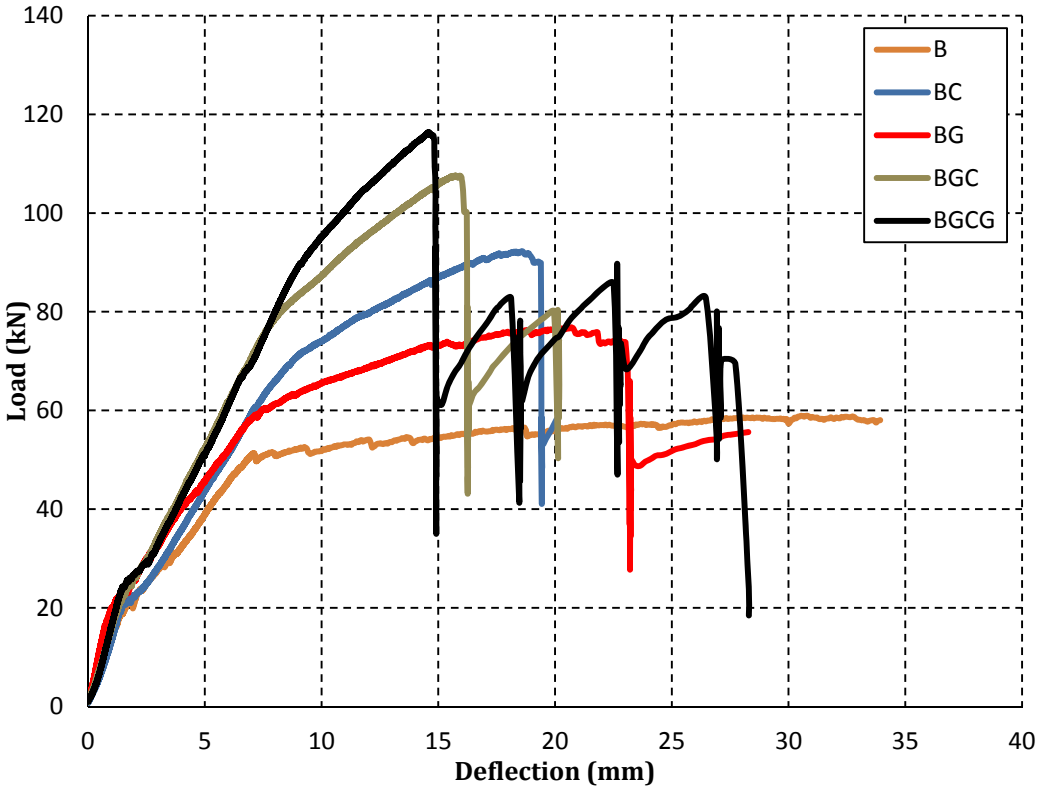

Fig. 4. Load versus Mid-Span Deflection